

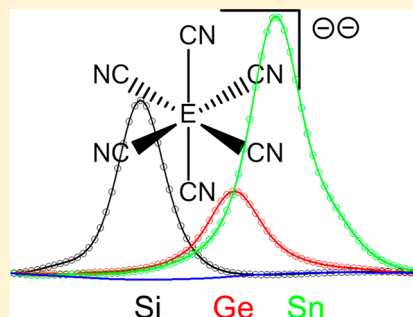
Syntheses, Structures, and Infrared Spectra of the Hexa(cyanido) Complexes of Silicon, Germanium, and Tin

Zoe M. Smallwood, Martin F. Davis, J. Grant Hill,^{1b} Lara J. R. James, and Peter Portius*^{1b}

Department of Chemistry, University of Sheffield, Brook Hill S3 7HF, United Kingdom

S Supporting Information

ABSTRACT: The rare octahedral EC₆ coordination skeleton type is unknown for complexes with coordination centers consisting of group 14 elements. Here, the first examples of such EC₆ species, the hexacoordinate homoleptic cyanido complexes E(CN)₆^{2−}, E = Si, Ge, Sn, have been synthesized from element halides SiCl₄, GeCl₄ and SnF₄ and isolated as salts with PPN counterions (PPN⁺ = (Ph₃P)₂N⁺) on a scale of 0.2–1 g. Characterization by spectroscopic techniques and by structure determination through single crystal crystallographic methods show that these pseudohalogen complexes have effective octahedral symmetry in solution and in the solid state. Infrared spectra obtained in solution reveal that the T_{1u} symmetric IR-active vibrations in all three complexes have unusually small oscillator strengths. The observed reluctance of Si(CN)₆^{2−}, Ge(CN)₆^{2−}, and Sn(CN)₆^{2−} to form from chloroprecursors was rationalized in terms of Gibbs free energies, which were found by ab initio calculations at the CCSD(T)-F12b/aug-cc-pVTZ(-PP)-F12 level of theory to be small or even positive. The work demonstrates that E(CN)₆^{2−} complexes of silicon, germanium and tin are in fact stable at room temperature and exist as well-defined units in the presence of noncoordinating counterions. The results add to our understanding of the chemistry of pseudohalogens and structure and bonding.



1. INTRODUCTION

Negatively charged cyanido, nitrate, cyanato, and azido molecules (Y[−]) among others, possess reactivity similar to that of halides. Birckenbach has rationalized this phenomenon by the concept of the pseudohalogen,^{1,2} which requires primarily that the Y[−] species form Y–Y dimers and Y–X inter pseudohalogens upon oxidation, have a stable protonated pro-ligand form H–Y and produce MY_n salts as well as EY_n^{q−} complexes. As demonstrated by the nonexistence of hexaazadiene that was proposed to be formed by the oxidation of N₃[−],^{3,4} not all pseudohalides fulfill the set of criteria completely.² Pseudohalogen complexes of the type EY_n^{q−} are isolable for most *p*-block elements in groups 13–15: Y = N₃ (B–Tl, Si–Sn, P–Bi), NCS (P, Si–Sn), NCO (Si, Ge, Sn), NO₃ (B, Al, Si–Sn). In group 14, they take the form of EL₄ and EL₆^{2−} (E = Si–Pb, L = N₃, NO₃, NCO, NCS, NCSe).^{5–12} However, there are only very few homoleptic cyanido complexes. This group of complexes is restricted to coordination centers of the less electronegative elements in groups 13 and 15 as P(CN)₃, Ga(CN)₄[−], E(CN)₅^{2−} (E = In, Tl, Sb, Bi) and Bi(CN)₆^{3−}.^{5–16} In group 14, the set of known complexes consist of the E(CN)₄ type (E = Ge, Sn), for which, apart from *in situ* ¹¹⁹Sn NMR spectral data for the Cl/CN ligand exchange to form Sn(CN)₆^{2−}, little analytical data is available.^{17–20} CN ligands possess a comparably low oxidation potential and this effects, for instance, the low thermal stability of P(CN)₅ which readily eliminates cyanogen at ambient temperature to form P(CN)₃.¹³ The related P(CN)₆[−] complex, on the other hand, is thought to be stabilized by hyper-

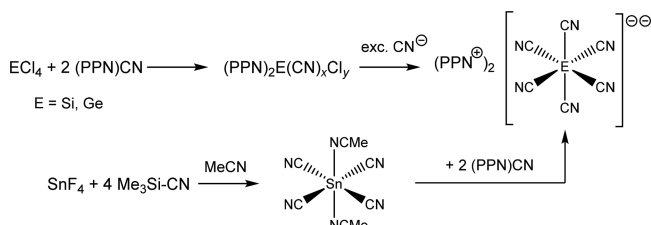
coordination. However, the synthesis of P(CN)₆[−] by means of conventional methods from (fluoro)phosphorus precursors is hampered by an affinity of P(CN)₅ toward F[−] (590 kJ mol^{−1}) that is vastly greater than that toward CN[−] (198 kJ mol^{−1}) and has, thus far, not been realized.¹⁴ Intriguingly, tetracyanosilane remains unknown despite numerous investigations into reactions involving silicon tetrahalides and cyanide salts.^{16,21,22} E(CN)₆^{2−} structures (E = Si–Pb) are interesting in general as they contain the octahedral EC₆ coordination skeletons which have hitherto, as opposed to the related covalent EC₆ networks in silicon carbide containing tetrahedral SiC₄ units,²³ not been reported (see ref 23 for related coordination geometries). Owing to the strength of the Si–C bonds [ΔH_d /(kJ mol^{−1}) = 318.0 to 338.9]²⁴ and the advantageous match of crystal and coordination geometries, SiC possesses great hardness and has found many applications due to this property.²³ Recently, germanium and tin complexes of the type E(Bu)R₂⁺ and Sn(R-2-py)₆²⁺ containing EC₆ coordination skeletons have been prepared with sterically hindered organic and other ligands. These are, however, either not octahedral or part of larger coordination networks.^{25,26} Using strategies involving exchange and transfer reactions employed previously for the synthesis of azido complexes,^{6,10,11} ionic and covalent cyanides were investigated as reagents for the formation of hexacyanido complexes of the type E(CN)₆^{2−} (E = Si, Ge, Sn), and the results are reported here.

Received: January 16, 2019

2. EXPERIMENTAL SECTION

The moisture sensitivity of starting materials for complexes **1**–**3** (ECl_4 or Me_3SiCN , see Scheme 1) necessitates the complete

Scheme 1. Reaction Sequences To Form $\text{PPN}_2\text{Si}(\text{CN})_6$ (1**), $\text{PPN}_2\text{Ge}(\text{CN})_6$ (**2**), and $\text{PPN}_2\text{Sn}(\text{CN})_6$ (**3**)^a**



^aFrom element halides via $[\text{E}(\text{CN})_x\text{Cl}_y]^{2-}$ intermediates ($x + y = 6$) and solvate $(\text{Sn}(\text{CN})_4(\text{MeCN})_2)$, **4a**; $\text{Sn}(\text{CN})_4(\text{py})_2$, **py** = pyridine, **4b**) complexes and $(\text{PPN})\text{CN}$, $\text{PPN}^+ = (\text{PPh}_3)_2\text{N}^+$.

exclusion of air, using standard Schlenk tube and inert gas box techniques. Extended experimental details are contained in the [Supporting Information](#), alongside all crystallographic information, spectra and other analytical details. The raw starting material bis(triphenylphosphine)iminium cyanide, $(\text{PPN})\text{CN}$, was prepared from $(\text{PPN})\text{Cl}$ and KCN according to Songstad et al.²⁷ However, the preparation of chlorine-free **1** relies on the complete absence of chlorine from the PPN starting material which was ensured by the removal of the KCl byproduct at an intermediate stage and the application of two batches of KCN in excess each time. **Caution!** $\text{PPN}(\text{CN})$ and the cyanido complexes **1**–**4** are toxic. The cyanido complexes hydrolyze readily; compounds **4a** and **4b** evolve hydrogen cyanide gas upon exposure to air.

2.1. Synthesis of $(\text{PPN})_2\text{Si}(\text{CN})_6$ (1**).** In a Schlenk tube, a solution of $(\text{PPN})\text{CN}$ (5.012 g, 8.88 mmol, 6.8 equiv) was prepared in the minimum amount of MeCN . SiCl_4 (0.15 cm^3 , 1.3 mmol, 1 equiv) was added, and the solution was stirred at 60 °C for 1 h, resulting in the formation of a small amount of white precipitate. After removal of the precipitate by filtration, the volume of the colorless filtrate was diminished *in vacuo* until the point of saturation was reached and the solution then cooled to –28 °C for 2 h, forming a white crystalline solid. The solid was collected by filtration, redissolved in MeCN , and then transferred into a new solution of $(\text{PPN})\text{CN}$ (1.000 g, 1.77 mmol, 1.35 equiv) in the same solvent. The reaction solution was heated as described above which, again, resulted in the formation of a small amount of white solid, attributed to some decomposition of a silicon-containing compound which was removed by filtration. As before, crystallization was achieved by evaporation of the filtrate *in vacuo* until a saturated solution was obtained at room temperature (r.t.) followed by lowering the temperature to –28 °C. This resulted in a white crop of large, colorless crystals consisting of pure $\text{PPN}_2\text{Si}(\text{CN})_6$ (**1**, 0.696 g, 42%). Mp 230–235 °C ($T_{\text{dec}} = 235$ °C). Anal. calcd for $\text{C}_{78}\text{H}_{60}\text{N}_8\text{P}_4\text{Si}$ (1261.35 g mol^{-1}): C 74.27, H 4.79, N 8.88%. Found: C, 74.22; H, 4.58; N, 8.66%. IR (nujol) $\bar{\nu}/\text{cm}^{-1} = 3470$ (br), 3056, 2696, 2612, 2592, 2584, 2221 (br), 2172, 2163, 2119, 2101, 1985, 1917, 1837, 1687, 1588, 1573, 1481, 1441, 1435, 1325, 1184, 1165, 1161, 1154, 1116, 1073, 1025, 998, 986, 932, 860, 850, 795, 763, 750, 746, 694, 663, 616, 583. ^{13}C NMR (CD_3CN) $\delta/\text{ppm} = 128.2$ (d, PPN), 130.3 (m, PPN), 133.2 (m, PPN), 134.5 (s, PPN), 139.9 (CN). IR (solution, MeCN) $\nu/\text{cm}^{-1} = 2182$, 2175, 2169, 2135. TOF MS ES(–) $m/z = 722$ ($[(\text{PPN})\text{Si}(\text{CN})_6]^-$, 100), 158 ($[\text{Si}(\text{CN})_5]^-$, 47), no signals were observed at 167 ($[\text{Si}(\text{CN})_5\text{Cl}]^-$) and 731 ($[(\text{PPN})\text{Si}(\text{CN})_5\text{Cl}]^-$ or any other Cl-containing species in the m/z range 75 to 900). Accurate masses (a.m.u.) found for $[\text{Si}(\text{CN})_5]^-$, $[(\text{PPN})\text{Si}(\text{CN})_6]^-$, 157.9921, 722.1806. Calcd: 157.9928, 722.1813. TOF MS ES(+), $m/z = 538$ ($[\text{PPN}]^+$, 100).

2.2. Synthesis of $(\text{PPN})_2\text{Ge}(\text{CN})_6$ (2**).** MeCN (20 mL) was added to $(\text{PPN})\text{CN}$ (3.142 g, 5.57 mmol, 6.32 equiv), resulting in almost

complete dissolution of all solid. To this stirred suspension was added GeCl_4 (0.10 cm^3 , 0.88 mmol, 1 equiv). The suspension was immersed into an oil bath and heated to 65 °C for approximately 41 h; after ~30 min of heating, only a small amount of solid (<100 mg) remained undissolved. The reaction mixture was allowed to cool to r.t. and settle and then the colorless supernatant solution was filtered off from a white filter residue (112 mg) that was discarded. The volume of the filtrate was the diminished *in vacuo* until the onset of precipitation occurred at which stage all solids were redissolved by warming the vessel in hot air. Crystallization was achieved at –25 °C. An initial crop of colorless crystals were obtained by filtration. The volume of the filtrate was further diminished and crystallization induced as described giving a second crop of colorless crystals which were shown to be spectroscopically identical to the first. Both crops were combined to give 2.210 g of mixture of $(\text{PPN})_2\text{Ge}(\text{CN})_6$, $(\text{PPN})\text{Cl}$, and $(\text{PPN})\text{CN}$. In order to complete the Cl/CN exchange, a mixture of a part of the combined crop (0.459 g, 0.35 mmol if $x = 5$), and NaCN (0.186 g, 3.80 mmol, 10.86 equiv), were suspended in MeCN (15 mL). After ~5 min stirring at r.t., the suspension had changed consistency owing to the dissolution of the germanium complex. The resultant reaction suspension was immersed in an oil bath set to a temperature of 65 °C. After a total of 196 h heating, the white suspension was filtered and the filter residue discarded. The colorless supernatant solution, containing the hexa(cyanido) complex was concentrated *in vacuo* until the onset of precipitation, warmed in hot air to redissolve all solids, and then placed in a freezer to induce crystallization. This gave colorless crystals which appear white in bulk under a pale yellow solution, which were collected by filtration to give pure $(\text{PPN})_2\text{Ge}(\text{CN})_6$ (**2**, 0.196 g, 82% with respect to GeCl_4) as colorless cuboidal crystals. Mp 188 °C (dec.). Anal. calcd for $\text{C}_{78}\text{H}_{60}\text{N}_8\text{P}_4\text{Ge}$ (1305.92 g mol^{-1}) C, 71.74; H, 4.63; N, 8.58; Ge, 0%. Found C, 71.37; H, 4.66; N, 8.63; Ge, <0.3%. IR (nujol) $\bar{\nu}/\text{cm}^{-1} = 3173$, 3145, 3079, 3063, 2251 (br), 2217 (br), 2165, 2159, 1985, 1918, 1906, 1824, 1780, 1684, 1613, 1588, 1575, 1482, 1439, 1436, 1316, 1301, 1284, 1265, 1185, 1162, 1116, 1109, 1073, 1027, 997, 795, 757, 750, 695, 689, 663, 617, 550, 534. ^1H NMR (400 MHz, CD_3CN , r.t.) $\delta/\text{ppm} = 7.45$ – 7.71 (m, PPN). ^{13}C NMR (100 MHz, CD_3CN , r.t., ppm) $\delta/\text{ppm} = 128.2$ (d, PPN), 130.3 (m, PPN), 133.2 (m, PPN), 134.6 (s, PPN), 140.0 (s, CN). IR (solution, MeCN) $\bar{\nu}/\text{cm}^{-1} = 2161$, 2135, 2089, 2080(sh), 2051. TOF MS ES(+) $m/z = 538$ ($[\text{PPN}]^+$, 100). TOF MS ES(–) $m/z = 245$ (100), 141(81), 123(17), spectra dominated by oxo(hydroxo) germanium species; no signals were attributable to $\text{Ge}_x(\text{CN})_y^{z-}$.

2.3. Synthesis of $\text{Sn}(\text{CN})_4(\text{MeCN})_2$ (4a**).** SnF_4 (0.261 g, 1.34 mmol, 1 equiv) was suspended in MeCN (15 mL). Me_3SiCN (0.67 mL, 5.36 mmol, 4.0 equiv) was added. After stirring at r.t. for ca. 17 h, a noticeably thicker white suspension had formed. The suspension was filtered, resulting in $\text{Sn}(\text{CN})_4(\text{MeCN})_2$ (0.234 g, 78%) as a white/cream solid filter residue. Anal. calcd for $\text{C}_8\text{H}_6\text{N}_6\text{Sn}$ (304.78 g mol^{-1}): C, 31.50; H, 1.98; N, 27.57%. Found C, 5.46; H, 0; N, 5.41. $\text{Sn}(\text{CN})_4(\text{MeCN})_2$ as well as $\text{Sn}(\text{CN})_4(\text{py})_2$ are extremely air sensitive and produce unreliable data. IR (nujol) $\bar{\nu}/\text{cm}^{-1} = 3320$ (br), 2321, 2289, 2241 (br), 2182, 1593 (br), 1260, 1207, 1169, 844, 804.

2.4. Synthesis of $(\text{PPN})_2\text{Sn}(\text{CN})_6$ (3**) from $\text{Sn}(\text{CN})_4(\text{MeCN})_2$ (**4a**).** A Schlenk tube was charged with a mixture of **4a** (0.209 g, 0.686 mmol, 1 equiv) and $(\text{PPN})\text{CN}$ (1.262 g, 2.24 mmol, 3.27 equiv) and then suspended in MeCN (15 mL). The tube was then immersed in an oil bath and the suspension stirred and heated to 60 °C for 21 h. After the reaction mixture had cooled to r.t., a small amount (<10 mg) of solid material was removed by filtration and discarded. The volume of the pale-yellow filtrate was diminished *in vacuo* until the onset of precipitation; any solids visible in the solution were redissolved by gentle heating and the resultant clear solution cooled to –28 °C. This resulted in an initial crop of yellow block-shaped crystals under a yellow supernatant solution, which was collected by filtration. Further reduction of the volume of the filtrate under vacuum resulted in a second crop of crystals which were spectroscopically identical to the first crop. The combined crops gave analytically pure **3** (0.914 g, 98% with respect to **4a**). Mp 271–275 °C. Anal.

Calcd for $C_{78}H_{60}N_8P_4Sn$ (1351.99 g mol⁻¹): C, 69.30; H, 4.47; N, 8.29; Cl, 0%. Found: C, 68.74; H, 4.54; N, 8.04; Cl, <0.3%. IR (nujol, cm⁻¹): $\bar{\nu}/\text{cm}^{-1}$ = 3173, 3146, 3081, 3064, 3039, 3025, 2794, 2787, 2696, 2252, 2218 (br), 2157, 2153, 2049 (br), 1985, 1915, 1833, 1616, 1588, 1575, 1482, 1439, 1436, 1260, 1252, 1186, 1179, 1114, 1069, 1028, 1020, 998, 941, 929, 924, 864, 797, 755, 695, 691, 664, 616, 550, 532. ¹H NMR (400 MHz, CD₃CN, r.t.) δ/ppm = 7.89–7.22 (m, PPN). ¹³C NMR (100 MHz, CD₃CN, r.t.) δ/ppm = 128.2 (dd, PPN), 130.3 (m, PPN), 133.2 (m, PPN), 134.6 (s, PPN), 138.5 (s, CN). IR (solution, MeCN) $\bar{\nu}/\text{cm}^{-1}$ = 2157, 2153 (sh), 2135. TOF MS ES(–), MeCN, m/z = 283 ([((NC)₂C₃N₃)₂Na][–], 100), 250 ([Sn(CN)₅][–], 33), 198 ([Sn(CN)₃][–], 20), 194 ([((NC)₂C₃N₃)Na(MeCN)][–], 22), 142 ([C₃N₃Na(MeCN)][–], 23). TOF MS ES(+), MeCN, m/z = 538 ([PPN]⁺, 100). No signals were observed at 259 ([Sn(CN)₄Cl][–]) and 207 ([Sn(CN)₂Cl][–]) or any other Cl-containing species.

3. RESULTS AND DISCUSSION

3.1. Syntheses. At 60–65 °C, solutions containing the group 14 chloride and the bis(triphenylphosphine)iminium cyanide (PPN)CN form mixed-ligand complexes of the type E(CN)_xCl_y^{2–} ($x + y = 6$) in which the distribution of chlorido(cyanido)complexes depends on the stoichiometric ratio of starting material (Scheme 1).

When crystallization is induced in the reaction mixture, the close chemical similarity of these E(CN)_xCl_y^{2–} complexes causes the formation of solid solutions. In the case of silicon, this finding is not only supported by crystallographic data (*vide infra*) but also by microanalytically determined CHN content in these crystals. At CN[–]/SiCl₄ starting material ratios of 2 and 10 mol mol⁻¹, the C, H, and N contents (% w/w) of 69.70, 4.22, and 5.43 and 72.98, 4.41, and 8.12, respectively, were found to be consistent to within $\pm 0.5\%$ with the empirical formulas Si(CN)_{2.9}Cl_{3.1}^{2–} and Si(CN)_{5.2}Cl_{0.8}^{2–}. This suggests that complete Cl/CN exchange requires molar ratios above 50 mol mol⁻¹, rendering this direct one-step method expensive. Since the (PPN)₂Si(CN)_xCl_y salts are separable from the reaction mixture by crystallization, decoordinates Cl[–] can be removed as (PPN)Cl and a supposed reaction equilibrium shifted toward Si(CN)₆^{2–} by exposing (PPN)₂Si(CN)_xCl_y to further amounts of (PPN)CN in a second step under otherwise identical conditions. After this treatment, the Cl content in the newly crystallized material had decreased to below 0.3% which translates to coefficients of $x > 5.9$ and $y < 0.1$. GeCl₄ and SnCl₄ also react with (PPN)CN to form chlorido(cyanido) complexes. However, in these cases the preparation of the Cl-free complexes is unfeasible due to an even less favorable position of the equilibrium. Instead, the intermediary (PPN)₂Ge(CN)_xCl_y was converted in the second step to (PPN)₂Ge(CN)₆ (2) by applying a large excess of NaCN instead of (PPN)CN and a longer reaction time (196 h). It was found that AgCN is not suitable as a CN-ligand transfer reagent since the crystallization from the solution containing (PPN)₂Ge(CN)_xCl_y and AgCN removes the PPN cation as part of the silver salt (PPN)Ag(CN)₂,²⁸ which was identified by single crystal XRD (see the Supporting Information, p 29). This reaction is also likely to occur if AgCN is used in syntheses of the Si and Sn analogs 1 and 3. SnCl₄ showed insufficient reactivity in the presence of either NaCN or (PPN)CN, hence, Sn(CN)₆^{2–} cannot be obtained by direct ligand exchange using ionic reagents. It was found that SnF₄ reacts readily with Me₃Si–CN in pyridine or acetonitrile under formation of the adducts Sn(CN)₄(L)₂ (L = MeCN, 4a; pyridine, 4b), which react further with (PPN)CN to afford

analytically pure (PPN)₂Sn(CN)₆ (3). The degree of progress of the halide/cyanide exchange reactions to all three E(CN)₆^{2–} complexes was established by C, H, N, and Cl elemental analyses and electrospray ionization mass spectrometry (see Figures S23–S25). The mass spectrum of 1 shows fragments corresponding to [(PPN)Si(CN)₆][–] at m/z = 722 and of [Si(CN)₅][–] at m/z = 158, but none at 731 and 167 that would correspond to a putative [Si(CN)₅Cl][–] species. Similarly, the signals detected of [Sn(CN)₅][–] and [Sn(CN)₃][–] in the spectra of 3 were free of accompanying masses that are likely to occur if Cl were still present. While the solid hexacyanido complexes are moderately air-sensitive, the solutions, especially those of 2 and 3, hydrolyze readily. Upon exposure to air, the decomposition of the solid white powders 4a and 4b also occurs rapidly and is accompanied by color change and the release of HCN. Even in hot polar solvent, the latter compounds are only sparingly soluble thus preventing further structural analysis.

3.2. Crystallographic Studies. Colorless cuboidal single crystals (1–3) suitable for single-crystal X-ray diffraction were obtained from hot, saturated MeCN solutions upon cooling to temperatures below –25 °C. X-ray diffraction studies performed on specimen of each of these types of crystals confirmed that in the three investigated reactions, hexacyanido complexes had formed as part of 2:1 salts with the PPN counterions: (PPN)₂E(CN)₆. This result allows for the structural analysis of the E(CN)₆^{2–} complexes of Si (1), Ge (2), and Sn (3) given below (see also the Supporting Information, p S9 ff). The EC₆ coordination skeletons of the investigated complexes adhere closely to the octahedral symmetry (Figures 1–3) with only small deviations in the

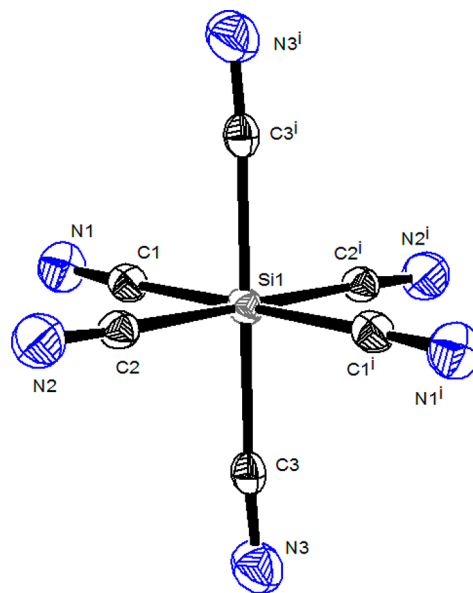


Figure 1. Thermal ellipsoid plots of the Si(CN)₆^{2–} complexes of 1 drawn at the 50% probability level; black, C; blue, N; gray, Si, “i” denotes symmetry-equivalent sites. Bond lengths [Å] and selected angles [°]: Si(1)–C(1) 1.9501(15), Si(1)–C(2) 1.9547(15), Si(1)–C(3) 1.9588(15), C(1)–N(1) 1.152(2), C(2)–N(2) 1.125(2), C(3)–N(3) 1.115(2); C(1)–Si(1)–C(2) 89.55(6), C(1)–Si(1)–C(3) 90.45(6), C(1)–Si(1)–C(3) 88.61(6), C(1)–Si(1)–C(3) 91.39(6), C(2)–Si(1)–C(3) 89.08(6), C(2)–Si(1)–C(3) 90.92(6), Si(1)–C(1)–N(1) 178.01(13), Si(1)–C(2)–N(2) 177.59(14), Si(1)–C(3)–N(3) 175.27(14).

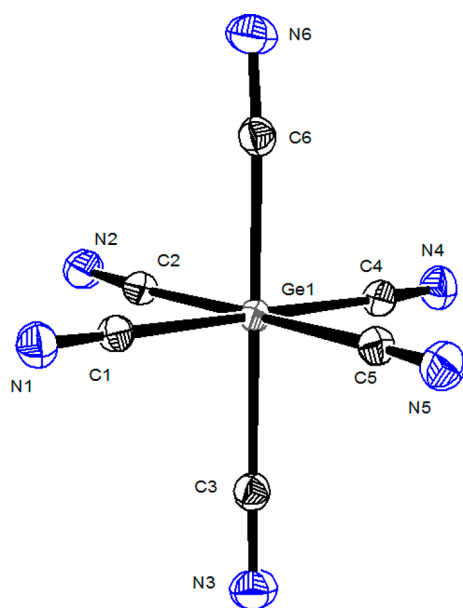


Figure 2. Thermal ellipsoid plots of the $\text{Ge}(\text{CN})_6^{2-}$ complex of **2** drawn at the 50% probability level; black, C; blue, N; gray, Ge. Bond lengths [Å] and selected angles [°]: Ge(1)–C(1) 2.0584(15), Ge(1)–C(2) 2.0441(15), Ge(1)–C(3) 2.0491(17), Ge(1)–C(4) 2.0480(15), Ge(1)–C(5) 2.0573(15), Ge(1)–C(6) 2.0407(16), C(1)–N(1) 1.1455(19), C(2)–N(2) 1.145(2), C(3)–N(3) 1.146(2), C(4)–N(4) 1.145(2), C(5)–N(5) 1.146(2), C(6)–N(6) 1.144(2); C(1)–Ge(1)–C(6) 90.99(6), C(2)–Ge(1)–C(5) 179.54(6), C(6)–Ge(1)–C(5) 91.5251(6), C(2)–Ge(1)–C(4) 89.97(6), C(6)–Ge(1)–C(4) 88.52(6), C(5)–Ge(1)–C(4) 89.8685(6), C(2)–Ge(1)–C(3) 91.85(6), C(6)–Ge(1)–C(3) 177.68(6), C(5)–Ge(1)–C(3) 88.58(6), C(4)–Ge(1)–C(3) 93.80(6), C(2)–Ge(1)–C(1) 89.92(6), C(6)–Ge(1)–C(1) 90.99(6), C(5)–Ge(1)–C(1) 90.25(6), C(4)–Ge(1)–C(1) 179.50(5), C(3)–Ge(1)–C(1) 86.70(6), N(1)–C(1)–Ge(1) 176.56(14), N(2)–C(2)–Ge(1) 174.12(14), N(3)–C(3)–Ge(1) 174.90(13), N(4)–C(4)–Ge(1) 174.92(13), N(5)–C(5)–Ge(1) 177.24(13), N(6)–C(6)–Ge(1) 176.14(13).

interligand angles of no more than 3.80(6) and 2.32(6)° from the ideal geometry of 90 and 180°, respectively, which is ascribed to the differences in the packing imposed by the crystal systems (**1**, orthorhombic; **2** and **3**, monoclinic, Figure 4). The cyanido ligands adopt the essentially linear end-on-C coordination ($\kappa(\text{C})$) mode that has been observed previously for other *p*-block complexes with coordination centers of groups 13 and 15.^{15,29} Structure models tested during crystallographic structure refinement that feature isocyanido ligands $\text{E}(\text{CN})_x(\text{NC})_y^{2-}$ all were significantly inferior in predicting the diffraction data, leading to substantially increased disagreement factors (*R*).

Within each $\text{E}(\text{CN})_6^{2-}$ complex, the lengths of C–N and E–C bonds vary only slightly at a level similar to that observed previously in crystals of $\text{K}_3\text{Fe}(\text{CN})_6$,²⁷ for instance (see Table 1). This variation is attributable to the crystal lattice-imposed, noncubic packing around the complex anions resulting in various sets of cation–complex anion contacts (Figure 4), rather than to electronic structure effects arising from the complexes themselves. It is a well-known fact that impurities in crystals may lead to deficiencies in crystal structure models (*vide supra*, discussion on intermediary chlorido(cyanide) species). Chlorine as the most likely candidate for forming solid solutions of the type $(\text{PPN})_2\text{E}(\text{CN})_x\text{X}_y$ ($x + y = 6$, X =

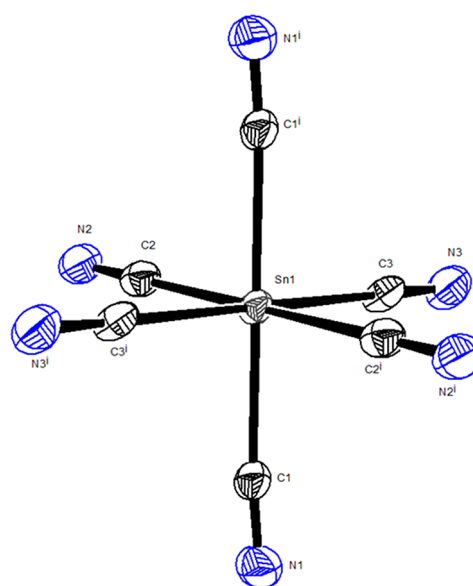


Figure 3. Thermal ellipsoid plots of the $\text{Sn}(\text{CN})_6^{2-}$ complex of **3** drawn at the 50% probability level; black, C; blue, N; gray, Sn, “i” denotes symmetry-equivalent sites. Bond lengths [Å] and selected angles: Sn(1)–C(3) 2.203(2), Sn(1)–C(1) 2.225(2), Sn(1)–C(2) 2.229(2), N(1)–C(1) 1.134(3), N(2)–C(2) 1.146(3), N(3)–C(3) 1.159(3); C(3)–Sn(1)–C(1) 91.65(8), C(3)–Sn(1)–C(2) 88.35(8), C(3)–Sn(1)–C(2) 88.43(8), C(3)–Sn(1)–C(2) 88.92(8), C(1)–Sn(1)–C(2) 91.08(8), C(3)–Sn(1)–C(2) 91.58(8), C(1)–Sn(1)–C(2) 88.92(8), N(1)–C(1)–Sn(1) 174.89(19), N(2)–C(2)–Sn(1) 175.73(19), N(3)–C(3)–Sn(1) 179.1(2).

Cl, and by implication similarly sized ligands), can be ruled out as sufficiently abundant contaminant. Support for this conclusion is found in the Cl contents of the substances used to grow the crystals for X-ray data collection, which were below the microanalytical detection limit (0.3%). This implies that the *x/y* ratio, which accounts for any Cl ligands potentially present in the crystals, is close to or above 5.9/0.1. Therefore, no more than one additional electron per formula unit is unaccounted for by a structure model that assumes *x/y* = 6/0 (further discussion of residual electron densities relating to Cl can be found in the Supporting Information). The system $(\text{PPN})_2\text{Si}(\text{CN})_x\text{Cl}_y$ ($x + y = 6$) is particularly prone to the formation of mixed crystals from solutions of incompletely Cl/CN-exchanged complexes, which results in residual electron density at distances from the coordination center typical for Si–Cl bonds in other hexacoordinate Si(IV) complexes (2.25–2.32 Å), but also in a reduction in the unit cell volume in line with typical crystallographic volumes of ligands ($y \sim 2.3$, $V = 6490.5(4) \text{ Å}^3$, $y < 0.1$, $V = 6662.7(2) \text{ Å}^3$, for details see the Supporting Information, p S9).

A comparison with the formula unit volumes found in the crystal structures of the related $\text{PPN}_2\text{E}(\text{N}_3)_6$ salts (all $P\bar{1}$ symmetry)^{6,10,11} reveals a trend, in which the $\text{E}(\text{CN})_6^{2-}$ complexes occupy consistently less space than $\text{E}(\text{N}_3)_6^{2-}$ complexes: $\Delta V/\text{Å}^3 = -28$ (Si), -66 (Ge), -50 (Sn).

3.3. Spectral Properties. Group theory requires isotopically pure octahedral $\text{E}(\text{CN})_6^{4-}$ complexes to exhibit only a single band in the region of the $\text{C}\equiv\text{N}$ stretches (ν_{CN}) of the IR spectrum due to the t_{1u} symmetric fundamental stretching vibrations. In MeCN solution, the hexacyanido complexes show this band at 2169 cm^{-1} (**1**), 2161 cm^{-1} (**2**), and 2157

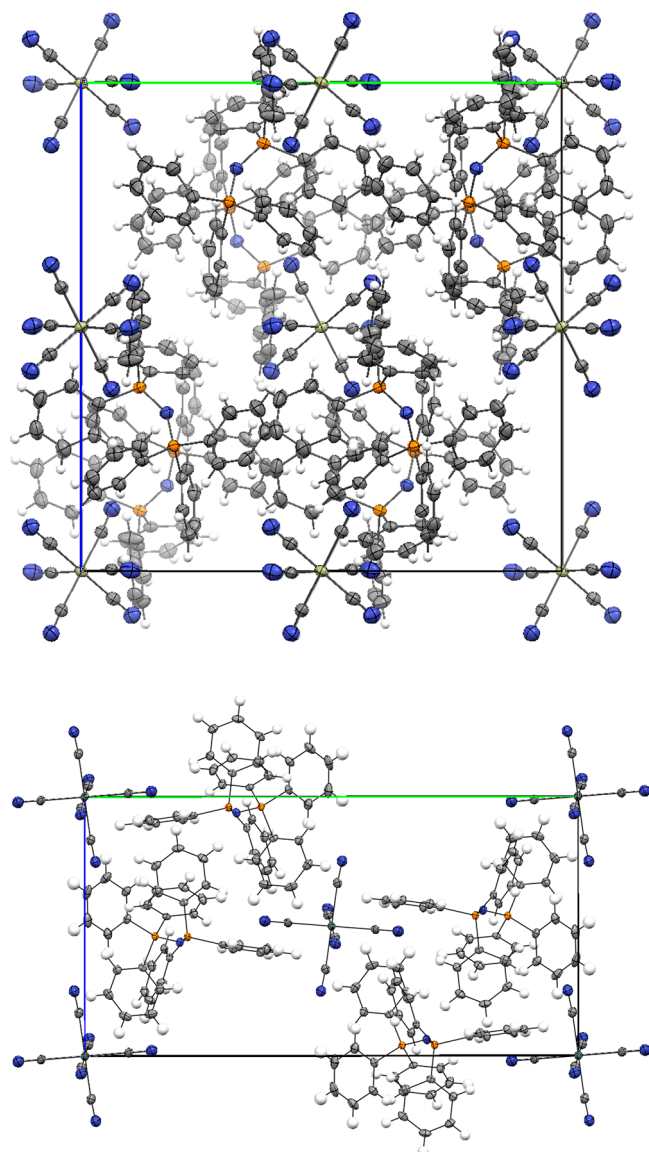


Figure 4. Projection of the unit cells of **1** (top) and **3** (bottom) down the crystallographic *a* axes; C, dark gray; N, blue; P, orange; Si, yellow; Sn, olive; H, light gray; ellipsoids set at the 50% level.

cm^{-1} (**3**), respectively (see Figure 5 bottom and Table 2). Compared to their azido analogues (see the references given above), the molar extinction coefficients of these bands are very small but still considerably larger than that of the CN^- anion itself at 2052 cm^{-1} in the same medium (see Figures S1–S13). The shift to higher wavenumbers in comparison to the latter is caused by electron donation from the σ^* orbital of

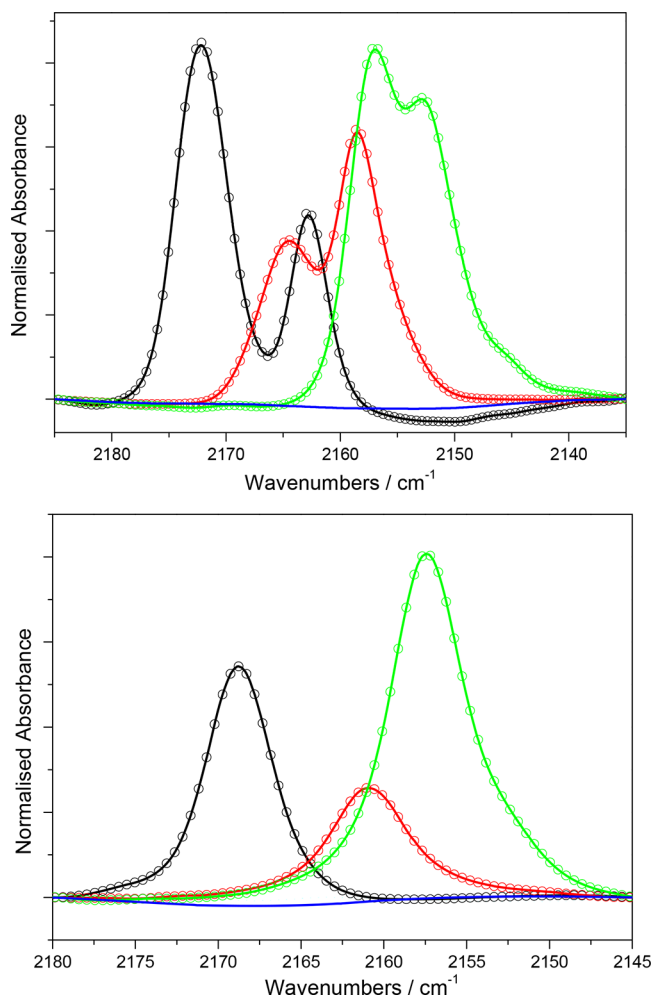


Figure 5. Transmission IR spectra of $(\text{PPN})\text{CN}$ (—), $\text{PPN}_2\text{Si}(\text{CN})_6$ (**1** ○), $\text{PPN}_2\text{Ge}(\text{CN})_6$ (**2** □), and $\text{PPN}_2\text{Sn}(\text{CN})_6$ (**3** △) between 2185 and 2135 cm^{-1} (top, mulls) and of MeCN solutions of $(\text{PPN})\text{CN}$ (4.0×10^{-2}), **1** (2.0×10^{-2}), **2** (1.0×10^{-2}), and **3** (9.9×10^{-3}) between 2180 and 2145 cm^{-1} (bottom, concentrations/mol dm^{-3} given in parentheses). The integrated intensities of those bands at 1186 cm^{-1} and $739\text{--}782\text{ cm}^{-1}$ attributed to the PPN cation were used for normalization.

the CN ligand and the ineffective back-donation into the π^* acceptor levels due to the lack of d-electrons at the coordination center. Compared to the related transition metal complexes $\text{Fe}(\text{CN})_6^{4-}$, $\text{Ti}(\text{CN})_6^{3-}$ and $\text{Fe}(\text{CN})_6^{3-}$, which display CN stretches at 2098 , 2071 , and 2135 cm^{-1} , respectively, those of the title complexes are, intriguingly, all at much higher frequencies and closer to those of the covalently bound tetracoordinate $\text{Me}_3\text{E-CN}$ cyanides at 2190 cm^{-1} ($\text{E} =$

Table 1. Key Structural Parameters of the $\text{E}(\text{CN})_6^{2-}$ Complexes of **1–3** in Comparison with $\text{K}_3\text{M}(\text{CN})_6$ ($\text{M} = \text{Cr}, \text{Fe}$) Derived from X-ray Diffraction Studies

compound	$d_{\text{C-N}}/\text{\AA}^a$	$d_{\text{E-C}}/\text{\AA}^a$	$\angle\text{E-C-N } \Delta_{\text{max}}/^\circ$	$\angle\text{C-E-C } \Delta_{\text{max}}/^\circ$	$\angle\text{C-E-C } \Delta_{\text{max}}/^\circ$	ref
$\text{E} = \text{Si}$ (1) ^b	1.115(2)–1.152(2)	1.950(2)–1.959(2)	4.7(1)	1.39(6)	± 0	^d
$\text{E} = \text{Ge}$ (2) ^c	1.144(2)–1.146(2)	2.041(2)–2.059(2)	5.9(1)	3.80(6)	2.32(6)	^d
$\text{E} = \text{Sn}$ (3) ^c	1.134(3)–1.159(3)	2.203(2)–2.229(2)	5.1(1)	1.65(8)	± 0	^d
$\text{K}_3\text{Fe}(\text{CN})_6$	1.131(22)–1.167(26)	1.927(14)–1.971(29)	8.6(1.5)	1.6(7)	± 0	30, 31
$\text{K}_3\text{Cr}(\text{CN})_6$	1.099(22)–1.167(17)	2.057(12)–2.100(10)	2.7(1.0)	1.1(5)	1.0(5)	32

^aMinimum–maximum values given. ^bData for 130 K. ^cData for 100 K. ^dThis work.

Table 2. Frequencies of the ν_{CN} Band Absorption Maxima Observed in the Transmission IR Spectra of Compounds 1–4 and (PPN)CN and Chlorido(cyano) Complexes

compound	solid ^{a,b}	solution ^{a,c}
(PPN)CN	2074, 2058, 2047	^e
(PPN) ₂ Si(CN) ₆ (1)	2172, 2163 (0.89) ^d	2168.8 (0.53, 4.74(6)) ^d
(PPN) ₂ Ge(CN) ₆ (2)	2164, 2159 (0.70) ^d	2160.8 (0.33, 5.64(6)) ^d
(PPN) ₂ Ge(CN) _x Cl _y	2155, 2053	
(PPN) ₂ Sn(CN) ₆ (3)	2157, 2153, 2146 (1) ^d	2157.3 (1, 5.68(9)) ^d
(PPN) ₂ Sn(CN) _x Cl _y	2157, 2153	
Sn(CN) ₄ (MeCN) ₂ (4a)	2182	^f
Sn(CN) ₄ (py) ₂ (4b)	2165	^f
Pb(CN) ₆ ²⁻		

^aFrequency at band maximum/cm⁻¹. ^bNujol mulls. ^cIn MeCN.

^dRelative ν_{CN} band area, ± 0.02 , and fwhm/cm⁻¹ in parentheses, areas based on compound 3 set to unity. ^eNot observed. ^fInsufficiently soluble.

Si, + 21 cm⁻¹),³⁴ 2181 cm⁻¹ (E = Ge, + 20 cm⁻¹),³⁵ and 2175 cm⁻¹ (E = Sn, + 18 cm⁻¹).^{36,37} This finding suggests that the E–C bonds are unusually strong and covalent despite the hypercoordinate character of the E(CN)₆²⁻ complexes. This conclusion is also reflected in the IR spectra of the complexes in the microcrystalline form where, however, additional ν_{CN} bands are present (Figure 5 top). Again, the analytically confirmed purity of each sample (*vide supra*) rules out any assignment to chlorido(cyano) species as components of a solid solution. The additional bands are more likely to be caused by the crystal packing-imposed symmetry at the sites of the E(CN)₆ complexes, which transforms with either the D_{2h} point group (1 and 3) or C_1 (2). Under D_{2h} , three fundamental ν_{CN} stretches of E(CN)₆ are IR-active (B_{1u} , B_{2u} , and B_{3u}). As these complexes have essentially octahedral geometry, their symmetry is closely related to D_{3d} and two of the three IR-active ν_{CN} stretches (A_{2u} and E_u) become degenerate so that only two absorption bands result, which aligns with the observations made in the spectra in the mull of 1 (D_{3h} , 2172 cm⁻¹ intense, 2163 cm⁻¹ medium) and 2 (D_{3h} , 2164 cm⁻¹ medium, 2159 cm⁻¹ intense), whereas the greater distortion of 3 produces three bands (D_{2d} , 2157 cm⁻¹ intense, 2153 cm⁻¹ intense, 2146 cm⁻¹ weak shoulder).

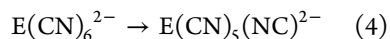
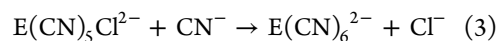
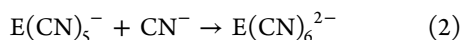
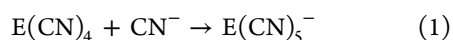
The frequency of the ν_{CN} stretch decreases from 1 to 3, a trend which matches that found in other pseudohalogen complexes such as E(N₃)₆²⁻ and in the series of Me₃E–CN compounds (E = Si, Ge, Sn, for refs see above). Due to their insolubility in inert solvents suitable for IR spectral investigation in the region of interest, spectra of 4a and 4b solutions were unattainable.

¹³C MAS NMR spectra were recorded of microcrystalline samples for all three hexacyanido complexes. The peaks arising from CN ligands could not be resolved due to overlap with the intense peaks of the PPN cations. ¹³C NMR spectroscopic studies of solutions of compound 1, however, display a well-resolved CN group resonance ($\delta(^{13}\text{C}) = 139.9$ ppm) with a chemical shift in between those of cyanosilanes, e.g., Me₃Si–CN (126.9 ppm),³⁸ and cyanide salts, e.g., (PPN)CN (166.5 ppm in the same solvent). Similar claims can be made for 2 and 3 (Me₃Ge–CN, 127.0 ppm;³⁹ Me₃Sn–CN, ~134 ppm).⁴⁰ ¹³C NMR spectra of dms-*d*₆ solutions of charge-neutral 4b, show a single resonance attributable to the CN ligands at $\delta = 113.8$ ppm, alongside the three signals of symmetrically coordinated pyridine ligands at 149.6, 136.1, and 123.9 ppm. To

corroborate the findings in solution, ¹³C–¹¹⁹Sn cross-polarization experiments were performed at 30 s delay time. However, under these parameters, only signals that belong to the PPN cation were observed, similar to those detected earlier by direct observation of ¹³C. Only minor differences between (PPN)Cl and the complexes are noticeable and signals of CN ligand(s) could not be attributed due to overlap of bands. ¹H T₁ measurements on (PPN)₂Sn(CN)₆ showed long relaxivity times of ~25 s. Therefore, it can be extrapolated that ¹⁵N and ¹³C will require extremely long acquisition times in the order of weeks and these were deemed unfeasible. A ¹⁵N MAS NMR spectrum for compound 3, obtained at a relaxation time of ~125 s, displayed only one very weak signal at ~362 ppm, which is assigned to the PPN cation.

While all attempts to observe the ²⁹Si and ⁷³Ge resonance of (PPN)₂Si(CN)₆ and (PPN)₂Ge(CN)₆ failed due to the lack of sensitivity of the spectrometer probe, the ¹¹⁹Sn MAS NMR spectrum of PPN₂Sn(CN)₆ displays a peak in the range of –600 to –1000 ppm, at $\delta(^{119}\text{Sn}) = -871$ ppm, which corresponds to the peak at ca. –879 ppm of the same compound in MeCN solution (¹J(¹¹⁹Sn, ¹³C) = 1218 Hz). The variance of $\delta(^{119}\text{Sn})$ with that published previously at –916.2 ppm²⁰ is large. The latter is the result of an assignment for *in situ* generated Sn(CN)₆²⁻ in CH₂Cl₂ solution; the authors state that Sn(CN)₆²⁻ could not be isolated. Given the independent, multiply verified identity and purity of the substance obtained as compound 3, and the similarity between MAS and solution ¹¹⁹Sn NMR spectra of this substance, we suggest that the previously observed chemical shift belongs to a Sn-containing species other than Sn(CN)₆²⁻ (see also Figures S14–S22).

3.4. Theoretical Studies. In order to rationalize the experimental findings, gas phase and solution energies of CN⁻, Cl⁻, E(CN)₄, E(CN)₅⁻, E(CN)₆²⁻, and E(CN)₅Cl²⁻ were calculated using density functional theory and coupled cluster methods (see the Supporting Information for full computational details). These energies are related to each other according to the reactions analogous to those evaluated by Haiges et al.¹⁵ (reactions 1–3) shown below. In view of earlier reports on trimethylsilylcyanide, which exists as an equilibrium mixture with the N-bonded silylisocyanide through a rapid CN group exchange reaction,³⁴ the relative stability of the linkage isomers E(CN)₅(NC)²⁻ was assessed relative to the homoleptic cyanido complexes, E(CN)₆²⁻ (E = Si–Sn) (reaction 4).



Geometry optimizations and harmonic frequency calculations were carried out at the PBE0 level of theory⁴¹ using the aug-cc-pV(T+d)Z basis set for C, N, Si, and Cl,⁴² where the “+d” denotes additional tight *d* functions for second row atoms, and the aug-cc-pVTZ-PP basis for the heavier atoms.⁴³ The latter is matched to small-core relativistic pseudopotentials replacing 10, 28, and 60 electrons for Ge, Sn and Pb, respectively. The complexes E(CN)₄, E(CN)₅⁻, E(CN)₅Cl²⁻ and E(CN)₆²⁻, E = Si–Pb, were optimized and were found to have *T_d*, *D_{3h}*, *C_{4v}* and *O_h* symmetry, respectively. Frequency calculations of the

Table 3. Observed (obs) and Calculated (calc) Bond Lengths ($d/\text{\AA}$) and Frequencies (ν/cm^{-1}) and Intensities of the CN Stretching Vibrations of the $\text{E}(\text{CN})_6^{2-}$ (a) and $\text{E}(\text{CN})_5(\text{NC})^{2-}$ (b) Complexes

		$\text{E}-\text{L}_{\text{obs}}^a$	$\text{E}-\text{L}_{\text{calc}}$	$\text{C}-\text{N}_{\text{obs}}^a$	$\text{C}-\text{N}_{\text{calc}}$	$\nu_{\text{CN}(\text{obs})}^b$	$\nu_{\text{CN}(\text{calc})}^c$
E = Si	(a)	1.956(10)	1.961	1.144(16)	1.156	2168.8 (0.53)	2281.8(0.08)
	(b)		1.957 ^d 1.863 ^e		1.156 ^d 1.166 ^e		2284.4(0.34) ^g 2202.6(207) ^h
E = Ge	(a)	2.052(7)	2.059	1.152(2)	1.156	2160.8 (0.33)	2277.2(0.02)
	(b)		2.048 ^d 1.999 ^e		1.156 ^d 1.166 ^e		2281.6(0.00) ^g 2194.0(195) ^h
E = Sn	(a)	2.222(14)	2.238	1.156(14)	1.157	2157.3 (1)	2276.0(1.57)
	(b)		2.227 ^d 2.168 ^e		1.156 ^d 1.167 ^e		2279.5(1.11) ^g 2191.5(193) ^h
E = Pb	(a)		2.329		1.157		2265.3(2.43)

^aThermal motion in the crystal may produce an apparent shrinkage of molecular dimensions and is considered by calculating instantaneous bond lengths D_i , which are estimated by $D_i \approx D_0 + |U_A - U_B|/D_0$ using the distances D_0 and thermal displacement parameters U_A , U_B for atoms A, B of the refined crystallographic structure solution; $\text{E}-\text{C}_{\text{obs}}$ and $\text{C}-\text{N}_{\text{obs}}$ are listed as unweighted mean x_u of D_i with either standard deviation $\sigma = [\sum(D_i - x_u)^2/(n-1)]^{0.5}$ or distribution of means $\sigma_m = \sigma_i/n^{0.5}$, whichever is larger, in parentheses; $n = 3$, Si, Sn; $n = 6$, Ge. ^bIn MeCN solutions, relative band areas in parentheses. ^cOscillator strength (in km mol^{-1}) given in parentheses. ^dCyanido ligands. ^eIsocyanido ligand. ^gE-symmetric C–N stretches. ^hIsocyanido C–N stretch.

minimum geometries obtained after optimization resulted in no imaginary frequencies (see the Supporting Information p S68). Bond lengths and angles derived from the calculated geometries for the $\text{E}(\text{CN})_6^{2-}$ complexes 1–3 and those observed crystallographically (Table 3) are within, or close to, the experimental 1σ uncertainty. Therefore, it is suggested that the PBE0/aug-cc-pV(T+d)Z(-PP) model is sufficiently reliable for predicting geometries and spectral properties, and can be used in conjunction with coupled cluster methods for energetics.

Remarkably, the $\text{C}\equiv\text{N}$ bond lengths are influenced only slightly by a change of the coordination center, which indicates that the electronic situation of the $\text{C}\equiv\text{N}$ bond is only marginally dependent on the central atom in group 14. The calculated vibrational frequencies and absorption cross sections validate the IR spectroscopic findings reported above suggesting that the transition dipole moments⁴⁴ of the IR-active T_{1u} -symmetric CN stretches have a minimum for $\text{Ge}(\text{CN})_6^{2-}$ and a maximum for $\text{Pb}(\text{CN})_6^{2-}$. The calculated frequencies for the isocyanido CN stretches in the hypothetical complexes of the type $\text{E}(\text{CN})_5(\text{NC})^{2-}$ (Si–Sn) are predicted to be about 80 cm^{-1} below those observed, and their absorption coefficients to be 3–4 orders of magnitude more intense than those of the cyanido ligands. In the recorded spectra, this region is free of such bands; therefore, we suggest that if isocyanido complexes are present in solution, then at a very low concentration.

Table 4 displays the net electronic energy changes for the reactions 1–3, as well as the correction terms for changes in the Gibbs free energies caused by thermal and solvent effects. As can be expected, the Lewis acid–base reactions of the attachment of a cyanido anion to the tetracoordinate tetracyano complex are highly exothermic, whereas the attachment of another cyanido ligand to form the hexacoordinate complexes is endothermic. While both types of reactions are endergonic at 298 K, solvent effects cause a large reduction in the Gibbs free energies so that according to the model used reactions 1 and 2 are spontaneous at r.t. for all evaluated coordination centers.

Since the synthesis of complexes 1–3 was investigated with ECl_4 as starting material (*vide supra*), it is the $\text{E}(\text{CN})_5\text{Cl}^{2-}$ complexes that are the ultimate intermediates to the hexacyano

Table 4. Reaction Energies (in kJ mol^{-1}) at 298 K for the Formation of the $\text{E}(\text{CN})_6^{2-}$ Complexes

E	reaction	$E_{\text{CCSD(T)}}^a$	$\Delta G_{\text{therm}}^b$	ΔG_{solv}^c	ΔG_{sol}^e
Si	1	−295.4	+48.4	+147.6	−99.3
	2	+26.5	+57.9	−176.9	−92.4
	3	−50.8	+18.2	+20.6	−12.0
	4				+4.4
Ge	1	−253.3	+45.5	+163.7	−44.1
	2	+60.2	+54.7	−159.9	−44.9
	3	−39.5	+17.6	+19.1	−2.8
	4				+12.5
Sn	1	−302.5	+42.8	+185.4	−74.2
	2	+20.6	+54.8	−133.0	−57.6
	3	−27.2	+17.0	+18.1	+7.9
	4				+10.2
Pb	1	−271.4	+40.3	+198.6	−32.5
	2	+48.9	+52.1	−114.1	−13.1
	3	−19.1	+16.5	+15.3	+12.7

^aGas-phase data at the CCSD(T)-F12b/aug-cc-pVTZ(-PP)-F12 level of theory using PBE0-optimized geometries. ^bthermodynamic Gibbs free energy (298 K) at the PBE0 level. ^cGibbs free energy of solvation in acetonitrile at the PBE0 level using the SMD approach. ^esolution-phase reaction energies.

complexes in the by Cl/CN exchange reactions. The solvent-effect-corrected Gibbs free energies for 298 K, the temperature at which 1–3 were isolated from the reaction solutions, clearly corroborate the experimentally observed trend in the reduction of the driving force for this reaction. On the basis of free Gibbs energies, ΔG_{solv} for solvated complexes, concentration ratios of $\text{E}(\text{CN})_6^{2-}/\text{E}(\text{CN})_5\text{Cl}^{2-}$ at 298 K can be calculated as 1.3×10^2 , 3.1, 4.1×10^{-2} , and 6.0×10^{-3} , respectively, which show that within this model reaction 3 to form $\text{Sn}(\text{CN})_6^{2-}$ from SnCl_4 with soluble ionic cyanides cannot be driven to completion. The ΔG_{sol} energies furthermore indicate a clear preference for homoleptic hexacyano complexes $\text{E}(\text{CN})_6^{2-}$ over their $\text{E}(\text{CN})_5(\text{NC})^{2-}$ linkage isomers.

CONCLUSION

Hexa(cyanido) complexes of the type $\text{E}(\text{CN})_6^{2-}$, E = Si, Ge, Sn, have been synthesized, isolated, and fully characterized as saltlike compounds with PPN counterions. The $\text{PPN}_2\text{E}(\text{CN})_6$

compounds are moderately air sensitive and dissolve readily in polar aprotic solvents without noticeable dissociation or linkage isomerization of the $\text{E}(\text{CN})_6^{2-}$ complex anions. The synthetic methodologies applied to these hypercoordinate complexes are partially based on those used previously for the N_3 , NCS and NCO analogues.^{6,8,45} However, more forcing conditions are required for the final reaction step $\text{E}(\text{CN})_5\text{Cl}^{2-} + \text{CN}^- \rightarrow \text{E}(\text{CN})_6^{2-} + \text{Cl}^-$, the reasons for which were identified with the help of systematic DFT and coupled cluster calculations. According to these calculations it is primarily the reduction in the net-loss of electronic energy in the reaction involving tin and, presumably, the similarity in Sn–CN and Sn–Cl bond strengths which cause the supposed reaction equilibrium to lie on the side of the starting material. Crystallographic studies have demonstrated that the CN ligands prefer the $\kappa(\text{C})$ -cyanido form in an only marginally distorted octahedral ligand sphere which demonstrates the viability of homoleptic octahedral complexes with the unusual EC_6 coordination skeletons in group 14.

■ ASSOCIATED CONTENT

● Supporting Information

The Supporting Information is available free of charge on the ACS Publications website at DOI: 10.1021/acs.inorgchem.9b00150.

Details of the crystallographic structure determination for compounds 1–3 and $((\text{PPN})\text{Ag}(\text{CN})_2)$, FTIR, NMR and mass spectra, Cartesian coordinates of the computational models and further preparative and experimental details (PDF)

Accession Codes

CCDC 1820145, 1820360, 1820362, and 1856451 contain the supplementary crystallographic data for this paper. These data can be obtained free of charge via www.ccdc.cam.ac.uk/data_request/cif, or by emailing data_request@ccdc.cam.ac.uk, or by contacting The Cambridge Crystallographic Data Centre, 12 Union Road, Cambridge CB2 1EZ, UK; fax: +44 1223 336033.

■ AUTHOR INFORMATION

Corresponding Author

*E-mail: p.portius@sheffield.ac.uk.

ORCID

J. Grant Hill: 0000-0002-6457-5837

Peter Portius: 0000-0001-8133-8860

Present Address

M.F.D.: Nanoco Technologies Ltd., Manchester M13 9NT, United Kingdom.

Notes

The authors declare no competing financial interest.

■ ACKNOWLEDGMENTS

This work was supported by the University of Sheffield; in particular, the authors thank the university for the award of a graduate teaching assistantship to ZS. The authors thank Prof. Wolfgang A. Herrmann (TU München) for his suggestions, Dr. Sandra van Meurs for recording NMR spectra and Harry Adams and Craig Robertson for their technical assistance in obtaining crystallographic data.

■ REFERENCES

- (1) Birckenbach, L.; Kellermann, K. Über Pseudohalogene (I). *Ber. Dtsch. Chem. Ges. B* **1925**, *58*, 786–794.
- (2) Golub, A. M.; Köhler, H.; Skopenko, V. V. *Chemistry of Pseudohalides*; Elsevier: New York, 1986.
- (3) Greschner, M. J.; Zhang, M.; Majumdar, A.; Liu, H.; Peng, F.; Tse, J. S.; Yao, Y. A New Allotrope of Nitrogen as High-Energy Density Material. *J. Phys. Chem. A* **2016**, *120*, 2920–2925.
- (4) Najafpour, J.; Foroutan-Nejad, C.; Shafiee, G. H.; Peykani, M. K. How does electron delocalization affect the electronic energy? A survey of neutral poly-nitrogen clusters. *Comput. Theor. Chem.* **2011**, *974*, 86–91.
- (5) Wiberg, E.; Michaud, H. Silicon tetraazide, $\text{Si}(\text{N}_3)_4$. *Z. Naturforsch., B: J. Chem. Sci.* **1954**, *9*, 500.
- (6) Filippou, A. C.; Portius, P.; Schnakenburg, G. The Hexaazidosilicate(IV) Ion: Synthesis, Properties and Molecular Structure. *J. Am. Chem. Soc.* **2002**, *124*, 12396–12397.
- (7) Seiler, O.; Burschka, C.; Goetz, K.; Kaupp, M.; Metz, S.; Tacke, R. The new λ^6 -Si-silicate dianion $[\text{Si}(\text{NCO})_6]^{2-}$ synthesis and structural characterization of $[\text{K}(18\text{-crown-6})]_2[\text{Si}(\text{NCO})_6]$. *Z. Anorg. Allg. Chem.* **2007**, *633*, 2667–2670.
- (8) Heininger, W.; Stucka, R.; Nagorsen, G. A new silicate anion: $[\text{Si}(\text{NCS})_6]^{2-}$. *Z. Naturforsch., B: J. Chem. Sci.* **1986**, *41*, 702–707.
- (9) Heininger, W.; Polborn, K.; Nagorsen, G. A further silicate anion: $[\text{Si}(\text{NCSe})_6]^{2-}$. *Z. Naturforsch., B: J. Chem. Sci.* **1988**, *43*, 857–861.
- (10) Filippou, A. C.; Portius, P.; Neumann, D. U.; Wehrstedt, K.-D. The Hexaazidogermanate(IV) Ion: Syntheses, Structures, and Reactions. *Angew. Chem., Int. Ed.* **2000**, *39*, 4333–4336.
- (11) Campbell, R.; Davis, M. F.; Fazakerley, M.; Portius, P. Taming Tin(IV) Polyazides. *Chem. - Eur. J.* **2015**, *21*, 18690–18698.
- (12) Portius, P.; Peerless, B.; Davis, M.; Campbell, R. Homoleptic Poly(nitrato) Complexes of Group 14 Stable at Ambient Conditions. *Inorg. Chem.* **2016**, *55*, 8976–8984.
- (13) Gall, H.; Schüppen, J. Über die Valenz-Grenze bei Phosphorcyaniden und Phosphorhordaniden. *Ber. Dtsch. Chem. Ges. B* **1930**, *63*, 482–487.
- (14) Bläsing, K.; Ellinger, S.; Harloff, J.; Schulz, A.; Sievert, K.; Täscher, C.; Villinger, A.; Zur Täscher, C. Lewis Acid Catalyzed Synthesis of Cyanidophosphates. *Chem. - Eur. J.* **2016**, *22*, 4175–4188.
- (15) Haiges, R.; Deokar, P.; Vasiliu, M.; Stein, T. H.; Dixon, D. A.; Christe, K. O. Preparation and Characterization of Group 13 Cyanides. *Chem. - Eur. J.* **2017**, *23*, 9054–9066.
- (16) Arlt, S.; Harloff, J.; Schulz, A.; Stoffers, A.; Villinger, A. Cyanido Antimonate(III) and Bismuthate(III) Anions. *Inorg. Chem.* **2016**, *55*, 12321–12328.
- (17) Menzer, W. Zur Kenntnis des Germaniumtetracyanids. *Angew. Chem.* **1958**, *70*, 656.
- (18) Jung, S.; Renz, F.; Klein, M.; Menzel, M.; Boča, R.; Stößer, R. Molecular switching in iron complexes bridged via tin-cyanides observed by Mössbauer and ESR spectroscopy. *J. Phys. Conf. Ser.* **2010**, *217*, 012027.
- (19) Bither, T. A.; Knoth, W. H.; Lindsey, R. V.; Sharkey, W. H. Trialkyl- and Triaryl(iso)cyanosilanes. *J. Am. Chem. Soc.* **1958**, *80*, 4151–4153.
- (20) Dillon, K. B.; Marshall, A. Tin-119 Nuclear Magnetic Resonance Studies of some Pseudohalogenoderivatives of $[\text{SnX}_6]^{2-}$ (X = Cl or Br). *J. Chem. Soc., Dalton Trans.* **1987**, 315–317.
- (21) Emerson, K. The preparation and structure of group V tricyanides. Ph.D. Thesis. University of Minnesota, Minneapolis, MN, 1960.
- (22) Howdeshell, J. P. The reactions of tris (trimethylsilyl) phosphine and attempted synthesis of silicon tetracyanide. Ph.D. Thesis. University of Wyoming, Laramie, WY, 1973.
- (23) Fan, J.; Chu, P. K.-H. Fabrication, Structure, Properties. In *Silicon Carbide Nanostructures. Engineering Materials and Processes*; Springer International Publishing: Switzerland, 2014.

- (24) Steele, W. C.; Nichols, L. D.; Stone, F. G. A. The Determination of Silicon-Carbon and Silicon-Hydrogen Bond Dissociation Energies by Electron Impact. *J. Am. Chem. Soc.* **1962**, *84*, 4441–4445.
- (25) Schrader, I.; Zeckert, K.; Zahn, S. Dilithium Hexaorganostannate(IV) Compounds. *Angew. Chem., Int. Ed.* **2014**, *53*, 13698–13700.
- (26) Yang, Y.; Panisch, R.; Bolte, M.; Müller, T. Bis-alkene Complexes of Stannylum and Germylium Ions. *Organometallics* **2008**, *27*, 4847–4853.
- (27) Martinsen, A.; Songstad, J. Preparation and properties of some bis(triphenylphosphine)iminium salts, $[(\text{Ph}_3\text{P})_2\text{N}]\text{X}$. *Acta Chem. Scand.* **1977**, *31a*, 645–650.
- (28) Jaafar, M.; Liu, X.; Dielmann, F.; Hahn, F. E.; Al-Farhan, K.; Alsalme, A.; Reedijk, J. Synthesis, structure and spectroscopic properties of bis(triphenylphosphane)iminium(chlorido) (cyanido) argentates(I). *Inorg. Chim. Acta* **2016**, *443*, 45–50.
- (29) Deokar, P.; Leitz, D.; Stein, T. H.; Vasilu, M.; Dixon, D. A.; Christe, K. O.; Haiges, R. Preparation and Characterization of Antimony and Arsenic Tricyanide and Their 2,2'-Bipyridine Adducts. *Chem. - Eur. J.* **2016**, *22*, 13251–13257.
- (30) Vannerberg, N.-G. The OD Structures of $\text{K}_3\text{Fe}(\text{CN})_6$ and $\text{K}_3\text{Co}(\text{CN})_6$. *Acta Chem. Scand.* **1972**, *26*, 2863–2876.
- (31) Shimanouchi, T.; Nakagawa, I. Infrared spectroscopic study on the co-ordination bond-II:I Infrared spectra of octahedral metal cyanide complexes. *Spectrochim. Acta* **1962**, *18*, 101–103.
- (32) Jagner, S.; Ljungstrom, E.; Vannerberg, N. G. The Crystal Structure of Potassium Hexacyanochromate(III), $\text{K}_3[\text{Cr}(\text{CN})_6]$. *Acta Chem. Scand.* **1974**, *28a*, 623–630.
- (33) Entley, W. R.; Treadway, C. R.; Wilson, S. R.; Girolami, G. S. The Hexacyanotitanate Ion: Synthesis and Crystal Structure of $[\text{NET}_4]_3[\text{Ti}^{\text{III}}(\text{CN})_6] \cdot 4\text{MeCN}$. *J. Am. Chem. Soc.* **1997**, *119*, 6251–6258.
- (34) Booth, M. R.; Frankiss, S. G. The constitution, vibrational spectra and proton resonance of trimethylsilyl cyanide and isocyanide. *Spectrochim. Acta, Part A* **1970**, *26*, 859–869.
- (35) Watari, F. Vibrational Spectra and normal coordinate calculations for $(\text{CH}_3)_3\text{GeCN}$ and $(\text{CD}_3)_3\text{GeCN}$. *J. Mol. Struct.* **1976**, *32*, 285–295.
- (36) Seyferth, D.; Kahlen, N. Trimethyl(iso)cyanogermane and trimethyltin (iso)cyanide. *J. Org. Chem.* **1960**, *25*, 809–812.
- (37) Lorberth, J. Preparation of organotin cyanides of the types R_3SnCN and $\text{R}_2\text{Sn}(\text{CN})_2$. *Chem. Ber.* **1965**, *98*, 1201–1204.
- (38) Arnold, D. E. J.; Craddock, S.; Ebsworth, E. a. V.; Murdoch, J. D.; Rankin, D. W. H.; Skea, D. C. J.; Harris, R. K.; Kimber, B. J. Nuclear Magnetic Resonance Spectra of Some Silyl and Trimethylsilyl Pseudo Halides. *J. Chem. Soc., Dalton Trans.* **1981**, 1349–1351.
- (39) Drake, J. E.; Glavincevski, B. M.; Humphries, R. E.; Majid, A. The carbon-13 chemical shifts of various methylgermanium derivatives. *Can. J. Chem.* **1979**, *57*, 1426–1430.
- (40) Brimah, A. K.; Siebel, E.; Fischer, R. D.; Davies, N. A.; Apperley, D. C.; Harris, R. K. Towards organometallic zeolites: Spontaneous self-assembly of Et_3SnCN , CuCN and $(^t\text{Bu}_4\text{N})\text{CN}$ to supramolecular $[(^t\text{Bu}_4\text{N})(\text{Et}_3\text{Sn})_2\text{Cu}(\text{CN})_4]$. *J. Organomet. Chem.* **1994**, *475*, 85–94.
- (41) Adamo, C.; Barone, V. Toward reliable density functional methods without adjustable parameters: The PBE0 model. *J. Chem. Phys.* **1999**, *110*, 6158–6170.
- (42) Dunning, T. H., Jr; Peterson, K.; Wilson, A. Gaussian basis sets for use in correlated molecular calculations. X. The atoms aluminum through argon revisited. *J. Chem. Phys.* **2001**, *114*, 9244.
- (43) Peterson, K. A. Systematically convergent basis sets with relativistic pseudopotentials. I. Correlation consistent basis sets for the post-d group 13–15 elements. *J. Chem. Phys.* **2003**, *119*, 11099–11112.
- (44) Gribov, L. A. The theory of intensities in the infrared spectra of polyatomic molecules. *Pure Appl. Chem.* **1969**, *18*, 339–351.
- (45) Portius, P.; Davis, M. A new hexakis(isocyanato)silicate(IV) and the first neutral Lewis-base adducts of silicon tetrakisocyanate. *Dalton Trans.* **2010**, *39*, 527–532.

NOTE ADDED IN PROOF

Since this work was submitted, a paper dealing with the synthesis and structure of $\text{Si}(\text{CN})_6^{2-}$ appeared online: Schulz, A.; Harloff, J.; Michalik, D.; Nier, S.; Stoer, P.; Villinger, A. Cyanidosilicates – Synthesis and Structure. *Angew. Chem. Int. Ed.*, <https://doi.org/10.1002/anie.201901173>.